Defects in flexible membranes with crystalline order

H. S. Seung and David R. Nelson

Lyman Laboratory of Physics, Harvard University, Cambridge, Massachusetts 02138

(Received 3 March 1988)

We study isolated dislocations and disclinations in flexible membranes with internal crystalline order, using continuum elasticity theory and zero-temperature numerical simulation. These defects are relevant, for instance, to lipid bilayers in vesicles or in the L_β phase of lyotropic smectic liquid crystals. We first simulate defects in flat membranes, obtaining numerical results in good agreement with plane elasticity theory. Disclinations and dislocations eventually exhibit a buckling transition with increasing membrane radius. We generalize the continuum theory to include such buckled defects, and solve the disclination equations in the inextensional limit. The critical radius at which buckling starts to screen out internal elastic stresses is determined numerically. Computer simulation of buckled defects confirms predictions of the disclination energies and gives evidence for a finite dislocation energy.

I. INTRODUCTION

The melting transition in two dimensions can be thought of as the destruction of crystalline order by proliferation of topological defects.[1,2] The mechanism of defect-mediated phase transitions involves a delicate balance between energy and entropy, first elucidated in a famous argument by Kosterlitz and Thouless.[1] They observed that a dislocation with Burgers vector b in a 2D (two-dimensional) crystal of radius R has an energy of order $K_0 b^2 \ln(R/a)$, where K_0 is the 2D Young's modulus and a is the lattice spacing. This energy cost suppresses the formation of dislocations at low temperatures. However, there is also an entropy of roughly $2k_B \ln(R/a)$ associated with a dislocation, since it can be located at $(R/a)^2$ possible positions. Above the critical melting temperature $k_B T_m \sim K_0 b^2$, the entropy term dominates, dislocations proliferate, and the crystal melts into a hexatic phase.[2] Another type of defect, the disclination, has an energy of order $K_0 s^2 R^2$, where s denotes the disclination charge. Its energy diverges so rapidly with system size that disclinations are not likely to occur naturally in 2D crystals.

In the general case of melting of *flexible* membranes, the balance between energy and entropy outlined above is upset. An arbitrary membrane is not confined to a plane, but instead may freely assume the shape of a general two-dimensional manifold. A simple physical example of such a system might be a large vesicle (lipid bilayer) brought below its 2D equilibrium freezing temperature,[3] or an L_β lyotropic smectic phase with the layers forced apart by the addition of water, in analogy to what has been accomplished already for lyotropic smectics with liquidlike in-plane order.[4] To describe the elastic properties of such systems, we must add a bending energy (which depends on the membrane's curvature) to the in-plane stretching energy.

A flexible membrane can relieve the strain field surrounding a defect by buckling out of the plane and trading stretching for bending energy. For example, we can create a positive disclination by cutting an angular sector out of a circular membrane and rejoining the edges of the cut.[5] If the membrane is constrained to a plane, rejoining these edges requires a great deal of stretching. But if the membrane is allowed to buckle into a cone, the strain field is "screened" out, and only a logarithmically divergent bending energy remains. Nelson and Peliti have argued that the energy of a buckled dislocation (which can be regarded as a tightly bound disclination pair) remains *finite* as the system size tends to infinity. Their argument predicts a finite density of unbound dislocations at any nonzero temperature; the membrane must melt, presumably into a hexatic phase.[6]

One can also approach the subject of topological defects in membranes from a different perspective, that of continuum elasticity theory. The elastic properties of a membrane are similar to those of an idealized thin plate of homogeneous isotropic material. Although the theory of thin plates was established long ago, almost all of its extensive literature is devoted to the special case of small deflections. Membranes with defects require a theory of large deflections, which is highly nonlinear and relatively unexplored. In addition, an understanding of the buckling behavior mentioned above requires the theory of elastic instability. These two elements of nonlinearity and buckling instability combine in an interesting way when applied to defects in membranes.

This paper begins with a review of results from plane elasticity theory. The energies of flat dislocations and disclinations are shown to be proportional to $\ln R$ and R^2, respectively. We then construct a numerical model of a flat membrane by defining a discrete stretching energy. Energies calculated using this model match the continuum theory prediction for the dislocation precisely. However, the disclination calculations expose an inaccuracy of the theory that is due to neglect of nonlinearities in the strain tensor. We derive continuum equations for buckled membranes with defects, following closely the theory

of thin plates.[7] The equations governing buckled disclinations can be solved exactly in the inextensional limit (infinite elastic constants), yielding energies proportional to $\ln R$. Through scaling arguments, the dependence of the buckling radius on the elastic parameters can be determined up to a proportionality constant. This constant can be calculated for disclinations and dislocations using an infinitesimal stability analysis formulated by Mitchell and Head.[8] We extend our numerical model to buckled membranes by defining a discrete bending energy. Comparison of numerical with analytic results for the disclination provides a valuable check of our numerical model. The energy of a buckled dislocation increases slower than any logarithmic divergence, and is probably finite. Note that *any* increase which is slower than logarithmic will lead to unbound dislocations at finite temperature, because the entropy in the Kosterlitz-Thouless argument still increases logarithmically.

II. CONTINUUM THEORY OF FLAT MEMBRANES

In plane elasticity theory, a deformation is represented by a displacement vector field $u(r) = (u_1, u_2)$, which maps the point $r = (x, y)$ to $r + u$. If there are no defects, the deformation is a single-valued mapping of the plane onto itself. In the presence of a dislocation, however, u becomes a multivalued function. Traversing any closed counterclockwise loop L containing the dislocation core increments u by a constant vector b, known as the Burgers vector.[7] In mathematical language,

$$\oint_L du_k = \oint_L \partial_i u_k \, dx_i = b_k \ . \tag{2.1}$$

Since the Burgers vector is always equal to some lattice vector, the multivaluedness of the displacement represents no physical ambiguity. If we express (2.1) in differential form, we see that derivatives of u do not commute, since

$$\epsilon_{li} \partial_l \partial_i u_j = b_j \delta(r - r_0) \ , \tag{2.2}$$

where r_0 is the location of the dislocation.

Disclinations are defined in terms of the bond angle field θ, which measures the orientation of bonds around each atom.[2] Traversing any closed loop L containing the disclination core increments θ by the "disclinicity" s,

$$\oint_L d\theta = \oint_L \partial_i \theta \, dx_i = s \ . \tag{2.3}$$

In a lattice with n-fold rotational symmetry, s must be some multiple of $2\pi/n$ to ensure that the multivaluedness of θ represents no physical ambiguity. We will be studying triangular lattices ($n = 6$) and small disclinicity, so the values $s = \pm 2\pi/6$ are most important. As before, the differential form of (2.3) is a statement about noncommutativity of derivatives,

$$\epsilon_{ij} \partial_i \partial_j \theta = s \delta(r - r_0) \ , \tag{2.4}$$

where r_0 now denotes the disclination location. Making the substitution

$$\theta = \tfrac{1}{2} \epsilon_{ij} \partial_i u_j \ , \tag{2.5}$$

which is valid for small $\partial_i u_j$, turns (2.4) into an equation involving displacements.

The stretching energy is taken to be quadratic in the strain,

$$F_s = \tfrac{1}{2} \int d^2 r (2\mu u_{ij}^2 + \lambda u_{kk}^2) \ , \tag{2.6}$$

where λ and μ are the two-dimensional Lamé coefficients, and indices run over the values 1 and 2. Although the exact form of the strain tensor is $u_{ij} = \tfrac{1}{2}(\partial_i u_j + \partial_j u_i + \partial_i u_k \partial_j u_k)$, for small displacements we may omit the terms quadratic in u_k, leaving

$$u_{ij} = \tfrac{1}{2}(\partial_i u_j + \partial_j u_i) \ . \tag{2.7}$$

If we minimize F_s with respect to variations in u, we obtain the equation

$$\partial_i \sigma_{ij} = 0 \ , \tag{2.8}$$

where the stress tensor σ_{ij} is defined by

$$\sigma_{ij} = 2\mu u_{ij} + \lambda u_{kk} \delta_{ij} \ . \tag{2.9}$$

Even though it would be possible to solve (2.8) for the vector displacements directly, it is more convenient to reformulate the problem in terms of a scalar potential, the Airy stress function χ.

Because σ_{ij} is symmetric and has zero divergence, it can be written as $\sigma_{ij} = \epsilon_{ik} \epsilon_{jl} \partial_k \partial_l \chi$, or, equivalently,[7,9]

$$\sigma_{xx} = \frac{\partial^2 \chi}{\partial y^2}, \quad \sigma_{yy} = \frac{\partial^2 \chi}{\partial x^2}, \quad \sigma_{xy} = -\frac{\partial^2 \chi}{\partial x \partial y} \ . \tag{2.10}$$

Although any choice for χ yields a stress tensor that satisfies Eq. (2.8), the choice cannot be arbitrary. For any physically realizable stress distribution, there must correspond some displacement vector field related to χ via

$$\tfrac{1}{2}(\partial_i u_j + \partial_j u_i) = u_{ij}$$
$$= \frac{1+\sigma}{K_0} \sigma_{ij} - \frac{\sigma}{K_0} \sigma_{ll} \delta_{ij}$$
$$= \frac{1+\sigma}{K_0} \epsilon_{im} \epsilon_{jn} \partial_m \partial_n \chi - \frac{\sigma}{K_0} \nabla^2 \chi \delta_{ij} \ . \tag{2.11}$$

The parameters K_0 and σ are the two-dimensional Young's modulus and Poisson ratio, and can be expressed in terms of the 2D Lamé coefficients,

$$K_0 = \frac{4\mu(\mu + \lambda)}{2\mu + \lambda} \ , \tag{2.12a}$$

$$\sigma = \frac{\lambda}{2\mu + \lambda} \ . \tag{2.12b}$$

We would like a constraint on χ which guarantees that (2.11) can be solved for the displacements. This constraint is easily found by applying $\epsilon_{ik} \epsilon_{jl} \partial_k \partial_l$ to both sides of (2.11), obtaining

$$\frac{1}{K_0} \nabla^4 \chi = \epsilon_{ik} \epsilon_{jl} \partial_k \partial_l u_{ij} = \epsilon_{ik} \epsilon_{jl} \partial_k \partial_l \tfrac{1}{2}(\partial_i u_j + \partial_j u_i) \ . \tag{2.13}$$

If the right-hand side of this equation vanishes, the strain

u_{ij} is said to be "compatible" with the existence of a single-valued displacement field, i.e., there exists some single-valued solution u_i of (2.11). If the right-hand side does not vanish, solutions of (2.11) must be multivalued. Hence the right-hand side is known as the "incompatibility," and $\epsilon_{ik}\epsilon_{jl}\partial_k\partial_l$ is known as an "incompatibility operator."[10,11]

Equation (2.13) can be transformed further into

$$\frac{1}{K_0}\nabla^4\chi = \epsilon_{ik}\epsilon_{jl}\partial_k\partial_l \tfrac{1}{2}(\partial_i u_j - \partial_j u_i)$$

$$+ \epsilon_{ik}\epsilon_{jl}\partial_k\partial_l\partial_j u_i$$

$$= \epsilon_{kl}\partial_k\partial_l\theta + \epsilon_{ik}\partial_k(\epsilon_{jl}\partial_l\partial_j u_i)$$

$$= \sum_\alpha s_\alpha\delta(\mathbf{r}-\mathbf{r}_\alpha) + \sum_\beta b_i^\beta\epsilon_{ik}\partial_k\delta(\mathbf{r}-\mathbf{r}_\beta) , \qquad (2.14)$$

where s_α denotes the disclination charge of a disclination at $\mathbf{r}_\alpha$, and $\mathbf{b}^\beta$ denotes the Burgers vector of a dislocation at $\mathbf{r}_\beta$. The microscopic origin of incompatibility is now manifest. The last line of (2.14) is simply the density of disclinations $s(\mathbf{r})$, if dislocations are thought of as disclination dipole pairs.[12] So 2D elasticity theory consists of just one equation, the biharmonic equation

$$\frac{1}{K_0}\nabla^4\chi = s(\mathbf{r}) . \qquad (2.15)$$

But solutions of this equation are not unique, for we may add any solution of the homogeneous equation. Without specification of boundary conditions on χ, the theory is still incomplete. We shall focus on the case of free boundary conditions, where the edges of the membrane are totally unconstrained. Then the body forces $P_i = \sigma_{ik}n_k$ (where $\mathbf{n}$ is the outward unit normal) must vanish on the edge of the membrane. This means that the components σ_{rr} and $\sigma_{r\phi}$ must be zero all along the boundary of a circular region.

For an isolated dislocation at the origin, Eq. (2.15) becomes

$$\frac{1}{K_0}\nabla^4\chi = b_i\epsilon_{ij}\partial_j\delta(\mathbf{r}) , \qquad (2.16a)$$

with solution[9,11]

$$\chi = \frac{K_0}{4\pi}b_i\epsilon_{ij}r_j\ln r . \qquad (2.16b)$$

To satisfy the boundary conditions on a finite region, we must add extra terms to (2.16b). However, these terms vanish in the limit of infinite system size, so we may neglect them. In other words, solution (2.16b) satisfies the boundary conditions at infinity, since the stresses $\sigma_{rr}, \sigma_{r\phi} \to 0$ like $1/r$ as $r \to \infty$. The energy of a dislocation is most conveniently evaluated by writing (2.6) in terms of the stress function,

$$F_s = \frac{1}{2K_0}\int d^2r(\nabla^2\chi)^2$$

$$- \frac{1+\sigma}{2K_0}\int d^2r\, \epsilon_{ik}\epsilon_{jl}\partial_k\partial_l(\partial_i\chi\partial_j\chi) . \qquad (2.17)$$

Substituting (2.16b) for χ and integrating, we find that

$$F_s = \frac{K_0 b^2}{8\pi}\ln\left[\frac{R}{a}\right] \qquad (2.18)$$

is the dislocation energy contained in the region $a \le r \le R$ of a membrane of infinite size. In the Kosterlitz-Thouless entropy argument, this formula was used to approximate the energy of a dislocation in a membrane of radius R.

The case of the disclination is more subtle, because we cannot so cavalierly neglect the boundary conditions. For an isolated disclination at the origin, Eq. (2.15) and its solution are[9]

$$\frac{1}{K_0}\nabla^4\chi = s\delta(\mathbf{r}) , \qquad (2.19a)$$

$$\chi = \frac{K_0 s}{8\pi}(Ar^2 + r^2\ln r) . \qquad (2.19b)$$

Without the homogeneous term Ar^2, (2.19b) would imply a strain on the boundary that diverges like $\ln R$. This is clearly unacceptable, for Eq. (2.6) is a harmonic approximation valid only for small strains. The material will of course fall apart if the strain diverges. Because of rotational symmetry,

$$\sigma_{r\phi} = -\frac{\partial}{\partial r}\left[\frac{1}{r}\frac{\partial\chi}{\partial\phi}\right]$$

vanishes identically for (2.19b). Requiring that

$$\sigma_{rr} = \frac{1}{r}\frac{\partial\chi}{\partial r} + \frac{1}{r^2}\frac{\partial^2\chi}{\partial\phi^2}$$

vanish at the boundary $r = R$ fixes the value of A,

$$A = -\tfrac{1}{2} - \ln R . \qquad (2.20)$$

The stress function is then

$$\chi = \frac{K_0 s}{8\pi}r^2\left[\ln\left[\frac{r}{R}\right] - \frac{1}{2}\right] , \qquad (2.21)$$

and the energy of the system is

$$F_s = \frac{K_0 s^2}{32\pi}R^2 . \qquad (2.22)$$

The fact that the $R \to \infty$ limit of (2.21) does not exist means that there is no solution of (2.19b) satisfying boundary conditions at infinity. The result (2.22) is not hard to understand. Because the strain field of an isolated disclination is roughly constant for large r, the stretching energy is simply proportional to the system size.[13]

It is worth noting that the situation is rather different for a charge neutral collection of disclinations with vanishing net Burgers moment. In this case, disclination charge and Burgers vector neutrality ensure that the net strain field decays to zero at large r, so A can be set to zero. The individual disclinations in the ensemble then interact with an $r^2\ln r$ potential.[14]

III. NUMERICAL SIMULATION OF FLAT MEMBRANES

We consider a 2D triangular lattice of atoms with unit mean spacing.[15] Any deformation maps the lattice points $\mathbf{r}_a$ into new locations $\mathbf{r}'_a$. We define a stretching energy

$$F_s^{\text{discrete}} = \tfrac{1}{2}\epsilon \sum_{\langle a,b \rangle} (|\mathbf{r}'_a - \mathbf{r}'_b| - 1)^2 , \qquad (3.1)$$

where the sum is over distinct nearest-neighbor pairs of atoms a and b. This can be reexpressed in terms of a stretching energy density U_a,

$$F_s^{\text{discrete}} = \tfrac{1}{2}\epsilon \sum_a U_a , \qquad (3.2)$$

where U_a is the local sum over nearest neighbors b of atom a,

$$U_a = \tfrac{1}{2}\sum_b (|\mathbf{r}'_a - \mathbf{r}'_b| - 1)^2 . \qquad (3.3)$$

To derive the continuum limit, imagine that some continuous deformation map $\mathbf{r}\rightarrow\mathbf{r}'$ is given which matches our discrete map $\mathbf{r}_a\rightarrow\mathbf{r}'_a=\mathbf{r}_a+\mathbf{u}_a(\mathbf{r}_a)$ at the lattice points. Let g_{ij} be the metric tensor induced by the deformation

$$g_{ij} = \partial_i \mathbf{r}' \cdot \partial_j \mathbf{r}' . \qquad (3.4)$$

Then we can make the approximation

$$
\begin{aligned}
|\mathbf{r}'_a - \mathbf{r}'_b| &\approx [g_{ij}(\mathbf{r}_a)r_{ab}^i r_{ab}^j]^{1/2} \\
&= \{[\delta_{ij} + 2u_{ij}(\mathbf{r}_a)]r_{ab}^i r_{ab}^j\}^{1/2} \\
&= [1 + 2u_{ij}(\mathbf{r}_a)r_{ab}^i r_{ab}^j]^{1/2} \\
&\approx 1 + u_{ij}(\mathbf{r}_a)r_{ab}^i r_{ab}^j ,
\end{aligned}
\qquad (3.5)
$$

since the strain tensor is defined by the equation $g_{ij}=\delta_{ij}+2u_{ij}$, and the undeformed distance $|\mathbf{r}_{ab}|$ is unity. As the index b ranges over the nearest neighbors of atom a in Eq. (3.3), the unit vector $\mathbf{r}_{ab}=\mathbf{r}_a-\mathbf{r}_b$ steps over the vertices $\mathbf{d}_\beta$ of a regular hexagon. This fact enables us to evaluate the stretching energy density

$$
\begin{aligned}
U_a &= \tfrac{1}{2}\sum_{\beta=1}^{6} (u_{ij}d_\beta^i d_\beta^j)^2 \\
&= \tfrac{3}{8}u_{ij}u_{kl}(\delta_{ij}\delta_{kl} + \delta_{ik}\delta_{jl} + \delta_{il}\delta_{jk}) \\
&= \tfrac{3}{8}(2u_{ij}^2 + u_{kk}^2) ,
\end{aligned}
\qquad (3.6)
$$

where the strain tensor is understood to be evaluated at $\mathbf{r}_a$. Thus the continuum limit of (3.2) becomes

$$F_s^{\text{discrete}} = \tfrac{1}{2}\epsilon \sum_a U_a \approx \frac{1}{\sqrt{3}}\epsilon \int d^2r\, U(\mathbf{r})$$

$$\approx \frac{\sqrt{3}}{8}\epsilon \int d^2r(2u_{ij}^2 + u_{kk}^2) . \qquad (3.7)$$

Comparing with (2.6), we can read off the 2D Lamé coefficients

$$\lambda = \mu = \frac{\sqrt{3}}{4}\epsilon , \qquad (3.8)$$

and calculate the 2D Young's modulus and Poisson ratio using (2.12),

$$K_0 = \frac{2}{\sqrt{3}}\epsilon, \quad \sigma = \tfrac{1}{3} . \qquad (3.9)$$

To construct membranes with defects, we start out with a hexagonal region of the lattice. The hexagon is composed of six equilateral triangular wedges. If we excise one wedge and attach the exposed edges, we obtain a positive disclination. The negative disclination is constructed by cutting a slit and inserting a seventh wedge. The dislocation is a hexagon with a line of atoms running from a vertex to the origin removed, or equivalently, a positive and negative disclination separated by a single lattice spacing. Sample configurations are depicted in Fig. 1.

In Sec. II we minimized the stretching energy functional $F_s[u_{ij}]$ to obtain the equations of plane elasticity theory. We have shown that the continuum limit of our function F_s^{discrete} of $2N$ coordinates (where N is the number of atoms) is precisely this functional. Hence minimizing F_s^{discrete} should give the same results for large N. There are two algorithms for minimization of a function which utilize gradient information: conjugate gradient and variable metric.[16] The conjugate gradient method is superior for our purposes because it requires less storage. Like most methods of multidimensional minimization, it is performed as a series of one-dimensional minimizations. Its special feature is that it constructs a series of "noninterfering," or "conjugate" directions. Minimiza-
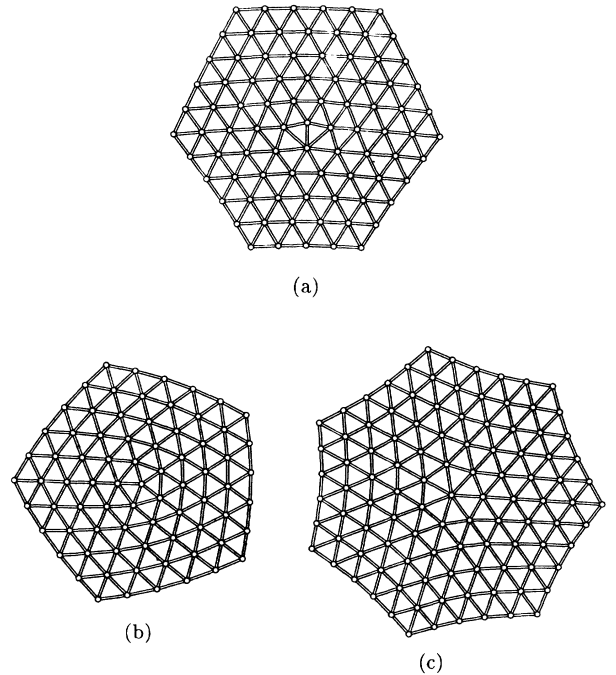

(a)

(b)

(c)

FIG. 1. (a) Flat dislocation. (b) Flat positive disclination ($s = 2\pi/6$). (c) Flat negative disclination ($s = -2\pi/6$).

tion along one direction does not "disturb" the effect of minimization in the other conjugate directions.

Figure 2 is a graph of F_s/K_0 versus R for flat dislocations with unit lattice spacing and Burgers vector. The semilogarithmic plot confirms the plane elasticity prediction (2.18), for it is linear with slope $1/8\pi$ to within 1% accuracy. The continuum limit is reached for surprisingly small system size. In Fig. 3 we see that $F_s/K_0 s^2 R^2$ for a flat disclination does indeed approach a constant, as predicted by Eq. (2.22). However, it approaches 0.0080, rather than the constant $1/32\pi = 0.0099$ following from (2.22). The discrepancy is due to two linearizing approximations made in plane elasticity theory: Eqs. (2.5) and (2.7) approximate the bond angle θ and the strain u_{ij} to be linear in the displacement. For dislocations, these formulas are accurate far from the defect core $(\partial_i u_j \sim b/r)$, but for disclinations they neglect terms of order $(\partial_i u_j)^2 \sim \text{const} \sim (1/6)^2$ for large r.

IV. CONTINUUM THEORY OF BUCKLED MEMBRANES

If we are to describe membranes which buckle out of the plane, we must add an extra function f to describe the "deflection." Then any deformed state is described by the displacement $\mathbf{u}(\mathbf{r}) = (u_1, u_2)$ and the deflection $f(\mathbf{r})$, which map the point $(x_1, x_2, 0)$ in the reference state to $(x_1 + u_1, x_2 + u_2, f)$.

The total energy is now a sum of stretching and bending contributions. The stretching energy F_s is the same as it was in the flat case (2.6), except that the expression
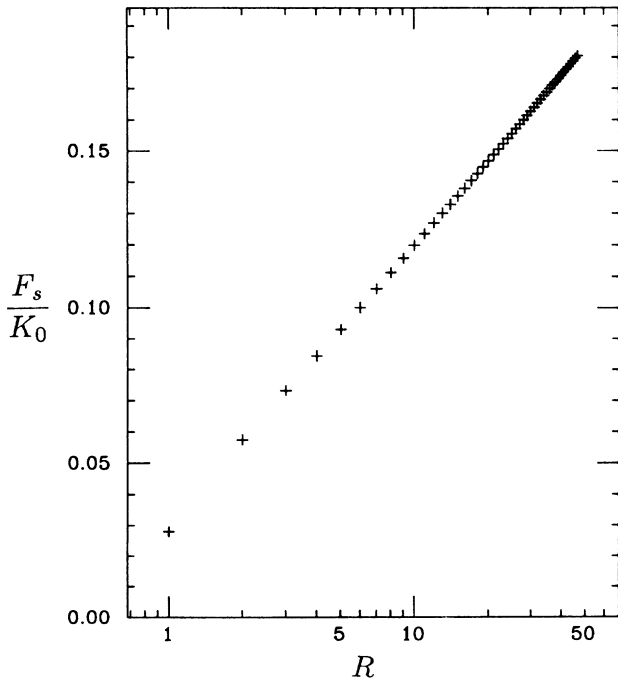

FIG. 3. Stretching energy (in units of $K_0 s^2$) divided by R^2 plotted vs R for disclinations.

(2.7) for the strain must be modified. The exact form of the strain tensor is $u_{ij} = \frac{1}{2}(\partial_i u_j + \partial_j u_i + \partial_i u_k \partial_j u_k + \partial_i f \partial_j f)$. For small displacement gradients, we may again omit the terms quadratic in u_k, leaving us with[7]

$$u_{ij} = \frac{1}{2}(\partial_i u_j + \partial_j u_i + \partial_i f \, \partial_j f) \ . \tag{4.1}$$

In much of the work done on the theory of plates, the term quadratic in f is also neglected. One is then left with the ordinary form of the strain tensor $u_{ij} = \frac{1}{2}(\partial_i u_j + \partial_j u_i)$ and thus a completely linearized theory. Since we will be concerned with the case of large deflections, we must retain the term quadratic in f, as there is no term of lower order in f.

The Helfrich bending energy of a membrane depends on its mean curvature H and Gaussian curvature K,

$$F_b = \int dS(\tfrac{1}{2}\kappa H^2 + \kappa_G K) \ , \tag{4.2}$$

where dS is the area element, κ the bending rigidity, and κ_G the Gaussian rigidity.[17] In terms of the deflection f, these curvatures are given by[18]

$$H = \nabla \cdot \left[\frac{\nabla f}{\sqrt{1 + |\nabla f|^2}} \right], \quad K = \frac{\det(\partial_i \partial_j f)}{(1 + |\nabla f|^2)^2} \ . \tag{4.3}$$

If $|\nabla f|$ is small, the forms

$$H \approx \nabla^2 f, \quad K \approx \det(\partial_i \partial_j f) = -\tfrac{1}{2}\epsilon_{ik}\epsilon_{jl}\partial_k \partial_l(\partial_i f \, \partial_j f) \tag{4.4}$$

are good approximations, and we can rewrite the bending energy as

FIG. 2. Semilogarithmic plot of stretching energy (in units of K_0) vs R for a flat dislocation with unit lattice spacing and Burgers vector.
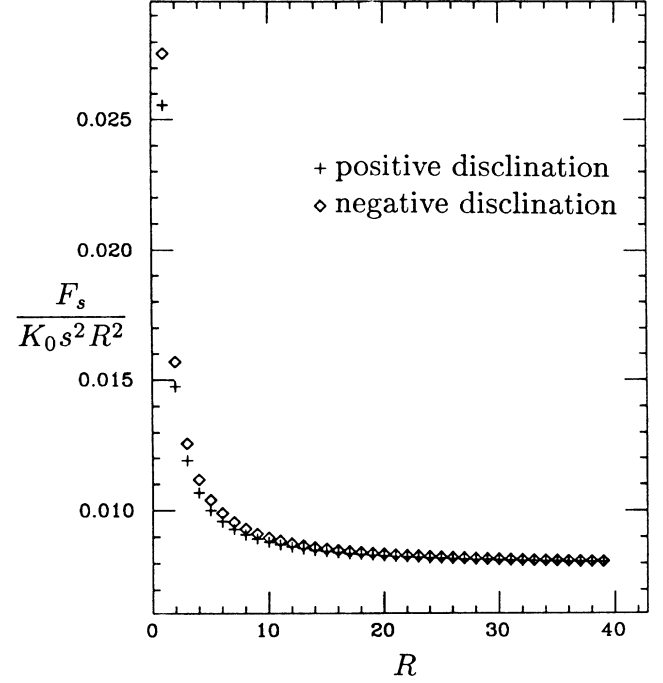
$$F_b \approx \tfrac{1}{2}\kappa \int d^2r (\nabla^2 f)^2 - \tfrac{1}{2}\kappa_G \int d^2r \, \epsilon_{ik}\epsilon_{jl}\partial_k\partial_l(\partial_i f \, \partial_j f) \; .$$

(4.5)

The total energy F is then the sum $F_b + F_s$ of the bending and stretching energies. An expression like (4.5) also emerges in the theory of thin plates, where κ and κ_G are expressed in terms of the bulk elastic constants.[7]

Taking variational derivatives of F with respect to $\mathbf{u}$ and f yields the equations

$$\kappa\nabla^4 f = \partial_i(\sigma_{ij}\partial_j f) \; ,$$

(4.6a)

$$\partial_i \sigma_{ij} = 0 \; ,$$

(4.6b)

where the stress tensor σ_{ij} is related to the nonlinear strain tensor as in Eq. (2.9). Again, we introduce the Airy stress function and derive an equation for it with the same manipulations used to obtain (2.14),

$$\frac{1}{K_0}\nabla^4\chi - \tfrac{1}{2}\epsilon_{ik}\epsilon_{jl}\partial_k\partial_l(\partial_i f \, \partial_j f)$$
$$= \sum_\alpha s_\alpha \delta(\mathbf{r}-\mathbf{r}_\alpha) + \sum_\beta b_i^\beta \epsilon_{ik}\partial_k \delta(\mathbf{r}-\mathbf{r}_\beta) \; .$$

(4.7)

Finally we can write a complete system of equations:

$$\kappa\nabla^4 f + \epsilon_{ik}\epsilon_{jl}\partial_k\partial_l(\partial_i\chi\,\partial_j f) = 0 \; ,$$

(4.8a)

$$\frac{1}{K_0}\nabla^4\chi = s(\mathbf{r}) - K(\mathbf{r}) \; ,$$

(4.8b)

where $s(\mathbf{r})$ and $K(\mathbf{r})$ are the disclination density and Gaussian curvature, respectively. Equation (4.8b) is almost the same as (2.15), except that the Gaussian curvature now acts like a source of disclinations and can "screen" out the stress. Since the Gaussian curvature term in (4.5) can be turned into an integral over the boundary, it affects not the equations on the interior but rather the boundary conditions. To our previous conditions $\sigma_{rr}, \sigma_{r\phi} = 0$ we must add

$$\frac{\kappa}{\kappa_G}\nabla^2 f + \left[\frac{1}{r}\frac{\partial f}{\partial r} + \frac{1}{r^2}\frac{\partial^2 f}{\partial\phi^2} \right] = 0 \; ,$$

(4.9a)

$$\frac{\kappa}{\kappa_G}\frac{\partial}{\partial r}\nabla^2 f - \frac{1}{r}\frac{\partial}{\partial r}\frac{1}{r}\frac{\partial^2 f}{\partial\phi^2} = 0 \; ,$$

(4.9b)

which must be satisfied on the boundary of a circular region.

When expanded in full, the equations become

$$\kappa\nabla^4 f = \frac{\partial^2\chi}{\partial y^2}\frac{\partial^2 f}{\partial x^2} + \frac{\partial^2\chi}{\partial x^2}\frac{\partial^2 f}{\partial y^2} - 2\frac{\partial^2\chi}{\partial x\,\partial y}\frac{\partial^2 f}{\partial x\,\partial y} \; ,$$

(4.10a)

$$\frac{1}{K_0}\nabla^4\chi + \frac{\partial^2 f}{\partial x^2}\frac{\partial^2 f}{\partial y^2} - \left[\frac{\partial^2 f}{\partial x\,\partial y}\right]^2$$
$$= \sum_\alpha s_\alpha \delta(\mathbf{r}-\mathbf{r}_\alpha) + \sum_\beta b_i^\beta \epsilon_{ik}\partial_k \delta(\mathbf{r}-\mathbf{r}_\beta) \; .$$

(4.10b)

For a defect-free membrane, the δ-function terms vanish, and we are left with the von Kármán equations for large deflections of thin plates.[19] These coupled nonlinear partial differential equations are "very complicated, and can-

not be solved exactly, even in very simple cases."[7]

For an isolated positive disclination at the origin, we assume rotational symmetry and write Eqs. (4.10) away from the disclination core as

$$\kappa\nabla^4 f = \frac{1}{r}\frac{d}{dr}\left[\frac{d\chi}{dr}\frac{df}{dr}\right] \; ,$$

(4.11a)

$$\frac{1}{K_0}\nabla^4\chi + \frac{1}{2r}\frac{d}{dr}\left[\frac{df}{dr}\right]^2 = 0 \; ,$$

(4.11b)

where

$$\nabla^2 = \frac{1}{r}\frac{d}{dr}r\frac{d}{dr} \; .$$

It is not difficult to guess a trial solution of these equations,

$$\chi = -\kappa \ln\left[\frac{r}{a}\right] \; ,$$

(4.12a)

$$f = \pm\left[\frac{s}{\pi}\right]^{1/2} r \; .$$

(4.12b)

With the help of Eqs. (4.1) and (2.9), the displacements u_x, u_y can now be calculated:

$$u_x = -\frac{s}{2\pi}y\phi - \frac{s}{2\pi}x + \frac{\kappa(1+\sigma)}{K_0}\frac{x}{r^2} \; ,$$

(4.13a)

$$u_y = \frac{s}{2\pi}x\phi - \frac{s}{2\pi}y + \frac{\kappa(1+\sigma)}{K_0}\frac{y}{r^2} \; ,$$

(4.13b)

where $\phi = \tan^{-1}(y/x)$. They in turn give a bond-angle field of $\theta = \tfrac{1}{2}\epsilon_{ij}\partial_i u_j = (s/2\pi)\phi$, which manifestly satisfies the integral condition (2.3). Performing the integral in (4.5), we obtain

$$F_b = s\kappa \ln\left[\frac{R}{a}\right]$$

(4.14)

for the bending energy.

Although it would appear that we have found an exact solution, comparison with the original form of the von Kármán equations (4.8) reveals that (4.12) is not a true solution because the left-hand side of Eq. (4.8b) is proportional to $\nabla^2\delta(\mathbf{r})$, while the right-hand side vanishes. If we attempt to bypass this issue by deleting a small disk of material around the origin, we create an inner boundary on which σ_{rr} and $\sigma_{r\phi}$ must vanish. One can easily calculate from the expression (4.12a) for χ that σ_{rr} behaves like $1/r^2$, so the inner boundary condition is badly violated if we excise a small disk.

Equations (4.12) are in fact an exact solution, but only for a limiting case, that of infinite elastic constants, $\mu, \lambda \to \infty$. This "inextensional" limit is exemplified by a piece of paper, which is free to bend, but is essentially impossible to stretch. Provided that χ remains finite, taking the limit $K_0 \to \infty$ eliminates the term $\nabla^4\chi / K_0$ from (4.8b) and leaves simply

$$\frac{\partial^2 f}{\partial x^2}\frac{\partial^2 f}{\partial y^2} - \left[\frac{\partial^2 f}{\partial x\,\partial y}\right]^2 = s(\mathbf{r}) \; .$$

(4.15)

Thus, the Gaussian curvature must exactly equal the dis-

clination density in the inextensional limit. The κ dependence of the inextensional equations can be scaled out by first writing (4.8a) in terms of χ/κ and f. The only parameter left is κ_G/κ, which enters through the boundary conditions. In the limit of infinite system size, this parameter has no effect either, provided that the derivatives of f in (4.9) fall off to zero. The bending energy must take the form

$$F_b = \kappa \Phi \left[\frac{\kappa_G}{\kappa}, R \right] , \qquad (4.16)$$

where Φ is a function that loses its κ_G/κ dependence in the large R limit. Since the stretching energy (2.17) vanishes in the inextensional limit, the total energy is just the bending energy. Equations (4.12) and (4.14) satisfy the inextensional equations, and exhibit the properties discussed above. The functions χ/κ, f, and F_b/κ are indeed independent of the elastic parameters, as expected in the limit of infinite system size.

To similarly solve for a negative disclination, we abandon the assumption of azimuthal symmetry, and write the von Kármán equations in general polar coordinates,

$$\kappa \nabla^4 f = \frac{\partial^2 \chi}{\partial r^2} \left[\frac{1}{r^2} \frac{\partial^2 f}{\partial \phi^2} + \frac{1}{r} \frac{\partial f}{\partial r} \right]$$
$$+ \frac{\partial^2 f}{\partial r^2} \left[\frac{1}{r^2} \frac{\partial^2 \chi}{\partial \phi^2} + \frac{1}{r} \frac{\partial \chi}{\partial r} \right]$$
$$- 2 \left[\frac{\partial}{\partial r} \left[\frac{1}{r} \frac{\partial \chi}{\partial \phi} \right] \right] \left[\frac{\partial}{\partial r} \left[\frac{1}{r} \frac{\partial f}{\partial \phi} \right] \right] , \qquad (4.17a)$$

$$\frac{1}{K_0} \nabla^4 \chi + \frac{\partial^2 f}{\partial r^2} \left[\frac{1}{r^2} \frac{\partial^2 f}{\partial \phi^2} + \frac{1}{r} \frac{\partial f}{\partial r} \right]$$
$$- \left[\frac{\partial}{\partial r} \left[\frac{1}{r} \frac{\partial f}{\partial \phi} \right] \right]^2 = s \delta(\mathbf{r}) . \qquad (4.17b)$$

A solution for the negative disclination of charge $-|s|$ when $K_0 \to \infty$ is given by

$$\chi = 3\kappa \ln \left[\frac{r}{a} \right] , \qquad (4.18a)$$

$$f = \frac{\sqrt{2|s|}}{3\pi} r \sin(2\phi) . \qquad (4.18b)$$

The displacements are most easily obtained by working in polar coordinates,

$$u_r = -\frac{|s|}{3\pi} r \sin^2(2\phi) , \qquad (4.19a)$$

$$u_\phi = -\frac{|s|}{2\pi} r [\phi + \tfrac{5}{12} \sin(4\phi)] . \qquad (4.19b)$$

The corresponding bond-angle field

$$\theta = \frac{1}{2r} \left[\frac{\partial}{\partial r} (r u_\phi) - \frac{\partial u_r}{\partial \phi} \right] = -\frac{|s|}{2\pi} [\phi + \tfrac{1}{4} \sin(4\phi)] \qquad (4.20)$$

correctly satisfies the integral condition (2.3). The bending energy is given by

$$F_b = 3 |s| \kappa \ln \left[\frac{R}{a} \right] . \qquad (4.21)$$

Unlike flat disclinations, buckled disclinations of equal and opposite charge do not have the same energy.

The case of the dislocation is very difficult. Because the equations are nonlinear, the simple tactic of superposing the solutions for positive and negative disclinations fails. Again, only in the inextensional limit do we have a chance of obtaining an analytic solution. We easily solved the disclination equations because all functions of the form $f = r\Psi(\phi)$ satisfy $K(r) \propto \delta(\mathbf{r})$. Similarly, the key to solving for the dislocation would be to find a class of functions which satisfy $K(\mathbf{r}) = b_i \epsilon_{ij} \partial_j \delta(\mathbf{r})$. Such functions (if they exist) remain unknown to us.

Recall that plane elasticity theory was a success for dislocations but only an approximation for disclinations. Similarly, Eqs. (4.10) are not likely to be quantitatively accurate for disclinations because $|\nabla f|$ is rather large. However, it is possible to determine the deformation of an inextensional positive disclination exactly. To insure a vanishing Gaussian curvature, we assume that the shape must be a generalized cone, i.e., have the form $f(r,\phi) = r\Psi(\phi)$. Furthermore, the angular factor $\Psi(\phi)$ must be equal to some constant α, by rotational symmetry. We fix α by requiring that the circumference of a unit disk missing a wedge of angle s equal the circumference of the base of the corresponding cone,

$$\alpha = \left[\frac{1}{\left[1 - \dfrac{s}{2\pi} \right]^2} - 1 \right]^{1/2} \approx 0.663 . \qquad (4.22)$$

Although this reduces to our previous result $\alpha = \sqrt{s/\pi}$ in the small s limit, for $s = \pi/3$ the estimate $\alpha \approx \sqrt{s/\pi} \approx 0.577$ is too low by about 9%.

The approximation (4.4) for the mean curvature is also in error, since $|\nabla f|$ is not small. Using the exact expression for the mean curvature given in (4.3) and the area element

$$dS = (1 + |\nabla f|^2)^{1/2} dx\, dy , \qquad (4.23)$$

the bending energy with $f = ar$ is then exactly

$$F_b = \tfrac{1}{2}\kappa \int dS\, H^2 = \frac{\alpha^2}{(1+\alpha^2)^{1/2}} \pi\kappa \ln \left[\frac{R}{a} \right]$$
$$= \left[\frac{1}{1 - \dfrac{s}{2\pi}} - \left[1 - \frac{s}{2\pi} \right] \right] \pi\kappa \ln \left[\frac{R}{a} \right]$$
$$\approx 1.152\kappa \ln \left[\frac{R}{a} \right] \quad \left[s = \frac{\pi}{3} \right] . \qquad (4.24)$$

In contrast, Eq. (4.14) gives $F_b \approx 1.047\kappa \ln(R/a)$.

Although we cannot solve the negative disclination exactly, we can derive a variational upper bound for the bending energy using the ansatz

$$f(r,\phi) = \beta r \sin(2\phi) . \qquad (4.25)$$

A geometric calculation analogous to that sketched above for the cone (this time with elliptic integrals) yields $\beta \approx 0.551$. The bending energy of this configuration is

$$F_b \approx 2.515\kappa \ln\left[\frac{R}{a}\right] , \tag{4.26}$$

which is an upper bound on F_b since the true solution is the one of minimum energy.

V. SCALING THEORY AND THE BUCKLING TRANSITION

So far, only in the limit of large K_0/κ and R do we know for certain that buckled disclinations exist. For both disclinations and dislocations, and any set of parameters, we would like to answer the following question: Does a buckled solution exist and is it stable? As we have seen for disclinations, the energy of a defect is less divergent for large R when it is buckled than when it is flat. Consequently our "phase diagram" should have a large R "buckled phase" separated from a small R "flat phase" by some critical buckling radius R_b.[8] We could also trigger the transition by holding R fixed and varying κ or K_0. The dependence of the buckling radius R_b on these elastic parameters can be determined almost completely through simple scaling arguments.

First of all, it will prove convenient to redefine the stress function to be $\tilde{X} = X/K_0$. Then the von Kármán equations (4.10) become

$$\frac{\kappa}{K_0}\nabla^4 f = \frac{\partial^2 \tilde{X}}{\partial y^2}\frac{\partial^2 f}{\partial x^2} + \frac{\partial^2 \tilde{X}}{\partial x^2}\frac{\partial^2 f}{\partial y^2} - 2\frac{\partial^2 \tilde{X}}{\partial x\,\partial y}\frac{\partial^2 f}{\partial x\,\partial y} , \tag{5.1a}$$

$$\nabla^4\tilde{X} + \frac{\partial^2 f}{\partial x^2}\frac{\partial^2 f}{\partial y^2} - \left[\frac{\partial^2 f}{\partial x\,\partial y}\right]^2 = s(\mathbf{r}) . \tag{5.1b}$$

It is evident from these equations and from the boundary conditions (4.9) that their solution $\psi = (\tilde{X}, f)$ depends only on the ratios K_0/κ and κ_G/κ. The displacements are obtained by solving an equation like (2.11),

$$\tfrac{1}{2}(\partial_i u_j + \partial_j u_i) = (1+\sigma)\epsilon_{im}\epsilon_{jn}\partial_m\partial_n\tilde{X} - \sigma\nabla^2\tilde{X}\delta_{ij}$$
$$- \tfrac{1}{2}\partial_i f\,\partial_j f . \tag{5.2}$$

Changing the Poisson ratio σ will change u_i but not $\tilde{X}$ or f.

Given a particular solution $\psi^* = (\tilde{X}^*, f^*)$ of (5.1) for some disclination density s^*, we can generate a whole class of related solutions via a simple rescaling procedure. We define new functions $f'(\mathbf{r}')$, $\tilde{X}'(\mathbf{r}')$, and $s'(\mathbf{r}')$ by

$$\mathbf{r}' = \lambda\mathbf{r}, \quad \tilde{X}'(\mathbf{r}') = \tau\tilde{X}^*(\mathbf{r}) ,$$
$$\tag{5.3}$$
$$f'(\mathbf{r}') = \sqrt{\tau}f^*(\mathbf{r}), \quad s'(\mathbf{r}') = \frac{\tau}{\lambda^4}s^*(\mathbf{r}) .$$

These new functions satisfy (5.1) and the boundary conditions (4.9) if K_0/κ is replaced by $K_0/\kappa\tau$. The rescaled disclination density corresponds to the following rescalings of Burgers vector and disclination charge:

$$\mathbf{b}' = \frac{\tau}{\lambda}\mathbf{b}, \quad s' = \frac{\tau}{\lambda^2}s . \tag{5.4}$$

For an isolated dislocation we can index every solution $\psi^* \equiv (\tilde{X}^*, f^*)$ by its Burgers vector $\mathbf{b}$, system size R, and parameters K_0/κ and κ_G/κ. Under the above rescaling procedure ψ^* is transformed into another solution $\psi' \equiv (\tilde{X}', f')$,

$$\psi^*\left[R, \frac{K_0}{\kappa}, \frac{\kappa_G}{\kappa}, b\right] \to \psi'\left[\lambda R, \frac{K_0}{\kappa\tau}, \frac{\kappa_G}{\kappa}, \frac{\tau}{\lambda}b\right] . \tag{5.5}$$

By choosing $\tau/\lambda = 1/b$ and $\tau = \kappa/K_0$, we can in fact relate all such solutions to a single reference solution with unit coupling ratio K_0/κ and unit Burgers vector b,

$$\psi^*\left[R, \frac{K_0}{\kappa}, \frac{\kappa_G}{\kappa}, b\right] \to \psi'\left[\frac{K_0 bR}{\kappa}, 1, \frac{\kappa_G}{\kappa}, 1\right] . \tag{5.6}$$

When the reference solution buckles at a critical value x_c of the ratio $K_0 bR/\kappa$, this instability must occur for the whole family of solutions. Therefore the critical buckling radius R_b must obey (dislocation)

$$R_b = x_c(\kappa_G/\kappa)\frac{\kappa}{K_0 b} , \tag{5.7a}$$

where x_c is a dimensionless function of the ratio κ_G/κ. A similar derivation for the disclination gives a critical buckling radius

$$R_b = y_c(\kappa_G/\kappa)\left[\frac{\kappa}{K_0|s|}\right]^{1/2} , \tag{5.7b}$$

where y_c is another dimensionless function.

Mitchell and Head have estimated x_c and y_c for $\kappa_G/\kappa = -0.7$.[8] They use two (basically equivalent) methods. First of all, infinitesimally close to the buckling transition, the von Kármán equations can be solved because nonlinear terms in f can be neglected. This method is only tractable in the simplest case of the positive disclination. The second method is to investigate the stability of the energy functional to infinitesimal perturbations about the flat defect solution. For this purpose they simply use the stress tensor of the flat defect. After expanding f in some basis set of functions, they are able to write the energy functional as a quadratic form in the coefficients of the expansion. The buckling radius R_b of a circular disk is determined by finding when the smallest eigenvalue of the quadratic form changes sign.

We have corrected errors in the Mitchell-Head analysis and carried it to higher order. The results for positive and negative disclinations are depicted in Fig. 4(a) for various values of κ_G/κ. Interestingly, each graph approaches zero for some value of κ_G/κ. To understand this behavior, recall that the buckling transition is due to the competing effects of two energies. The bending energy tends to stabilize the flat solution, while the stretching energy makes it unstable. For certain values of κ_G/κ, the bending energy also becomes unstable, which means that there is nothing to prevent buckling at any system size. In terms of the principal curvatures c_1 and c_2 the Helfrich energy takes the form
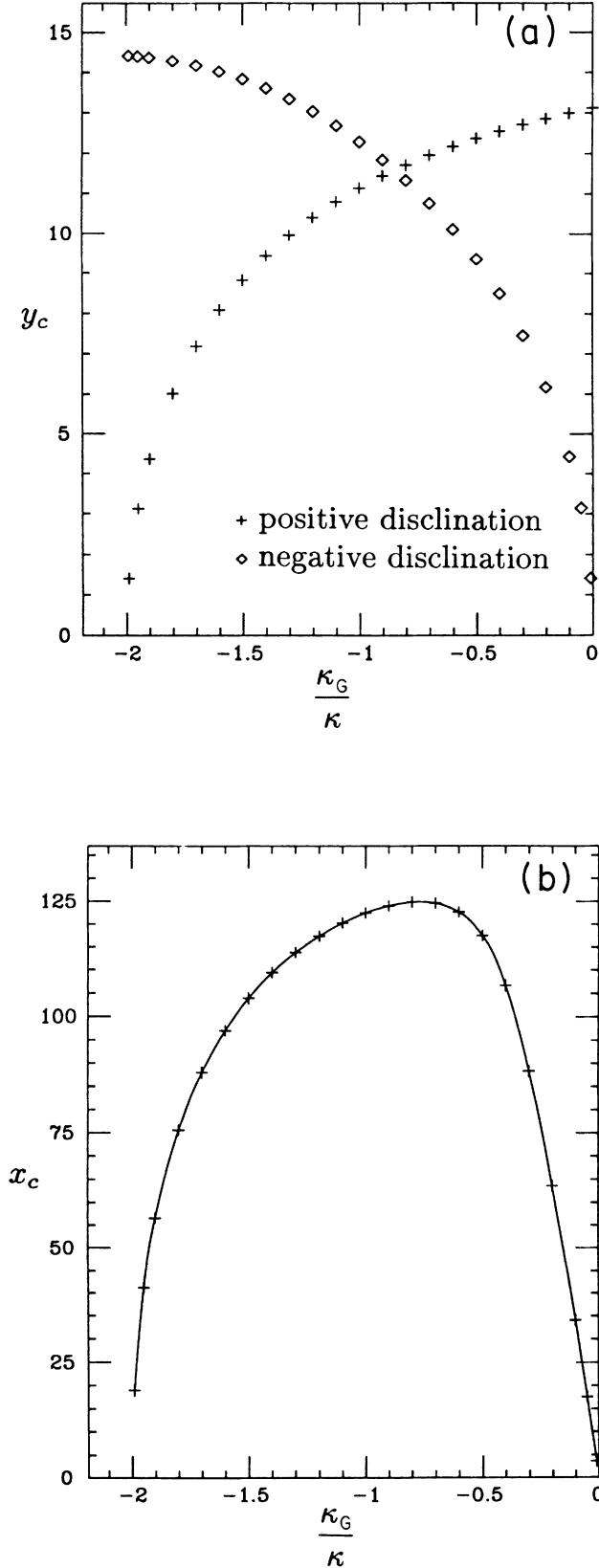
FIG. 4. (a) Scaling function y_c vs κ_G/κ for positive and negative disclinations. (b) Scaling function x_c vs κ_G/κ for a dislocation.

$$F_b = \kappa \int dS \left[\tfrac{1}{2}(c_1 + c_2)^2 + \frac{\kappa_G}{\kappa} c_1 c_2 \right] . \tag{5.8}$$

When $\kappa_G/\kappa > 0$, the Helfrich energy is unstable to deflections with $c_1 = -c_2$. This instability should apply to the negative disclination, since its buckled shape has negative Gaussian curvature. We can also write the Helfrich energy as

$$F_b = \kappa \int dS \left[\frac{1}{2}(c_1 - c_2)^2 + \left(\frac{\kappa_G}{\kappa} + 2 \right) c_1 c_2 \right] . \tag{5.9}$$

When $\kappa_G/\kappa + 2 < 0$, the energy is unstable to a deflection with $c_1 = c_2$. We would expect this instability to apply to the positive disclination. From Fig. 4(b) we can see that the dislocation buckling radius is zero at both $\kappa_G/\kappa = 0$ and $\kappa_G/\kappa = -2$. This is because the dislocation is just a pair of disclinations, and the buckling behavior of each disclination dominates at each end of the interval.

The Mitchell-Head calculations are approximate in that they use a truncated set of basis functions. However, the calculations converge fairly well as the basis is made larger and larger, so this is not so great a limitation. A more serious deficiency is that the disclination calculation utilizes expression (2.19b) for the stress, which is somewhat inaccurate as discussed previously. Linear stability analysis will, moreover, only produce an upper bound on the critical buckling radius unless the instability proceeds as a kind of "second-order" transition. It is possible that for some choices of parameters, there exist flat and buckled solutions which are both infinitesimally stable, and that a "first-order" buckling transition precedes the instability of Mitchell and Head.

In Sec. VI, the buckling transition will be studied numerically. For purposes of comparison, we list our estimates of the buckling radii for $\kappa_G/\kappa = -1$:

positive disclination,

$$R_b \left[\frac{K_0 s}{\kappa} \right]^{1/2} \lesssim 11.1 \tag{5.10a}$$

negative disclination,

$$R_b \left[\frac{K_0 |s|}{\kappa} \right]^{1/2} \lesssim 12.3 \tag{5.10b}$$

dislocation,

$$R_b \frac{K_0 b}{\kappa} \lesssim 122 . \tag{5.10c}$$

Inequalities are used as a reminder that these estimates are stability limits for a possibly "first-order" buckling transition.

VI. NUMERICAL SIMULATIONS OF BUCKLED MEMBRANES

We consider the same 2D triangular lattice as in the flat case, except that we allow it to bend. The total energy is $F = F_s^{\text{discrete}} + F_b^{\text{discrete}}$, where F_s^{discrete} is given by (3.1), and the bending energy F_b^{discrete} is a function of the unit normals to every elementary triangle,[20]

$$F_b^{\text{discrete}} = \tfrac{1}{2}\tilde{\kappa} \sum_{\langle \alpha,\beta \rangle} |\mathbf{n}_\alpha - \mathbf{n}_\beta|^2$$

$$= \tilde{\kappa} \sum_{\langle \alpha,\beta \rangle} (1 - \mathbf{n}_\alpha \cdot \mathbf{n}_\beta) . \tag{6.1}$$

The sum is over nearest-neighbor pairs of normals $\mathbf{n}_\alpha$ and $\mathbf{n}_\beta$, and the normals have been assigned with a consistent choice of orientation. To derive the continuum limit, we suppose that the shape of the membrane is parametrized by the map $\mathbf{x}(\sigma_i)$ $(i = 1,2)$. The coordinate frame for the surface is given by $\mathbf{e}_i = \partial_i \mathbf{x}$, the induced metric by $g_{ij} = \mathbf{e}_i \cdot \mathbf{e}_j$, and the second fundamental form by $\Omega_{ij} = \mathbf{e}_i \cdot \partial_j \mathbf{n}$.[18] In the continuum limit the difference $\mathbf{n}_\alpha - \mathbf{n}_\beta$ should become the gradient of the normal vector field,

$$F_b = \tfrac{1}{2}\kappa \int dS\, g^{ij} \partial_i \mathbf{n} \cdot \partial_j \mathbf{n} . \tag{6.2}$$

Substituting $\partial_i \mathbf{n} = \Omega_i^k \mathbf{e}_k$ allows us to express the bending energy in terms of Ω_{ij},

$$F_b = \tfrac{1}{2}\kappa \int dS\, g^{ij} g^{kl} \Omega_{ik} \Omega_{jl} . \tag{6.3}$$

Using the identity $\epsilon^{il}\epsilon_{jk} = \delta_j^i \delta_k^l - \delta_k^i \delta_j^l$, or, equivalently,

$$g^{ij}g^{kl} = g^{ik}g^{jl} + \epsilon^{il}\epsilon_{mn}g^{mj}g^{nk} , \tag{6.4}$$

we rewrite the integrand of (6.3) as

$$g^{ij}g^{kl}\Omega_{ik}\Omega_{jl} = (g^{ik}\Omega_{ik})^2 + \epsilon^{il}\epsilon_{mn}g^{mj}\Omega_{jl}g^{nk}\Omega_{ik}$$

$$= (\Omega_i^i)^2 + \epsilon^{il}\epsilon_{mn}\Omega_l^m\Omega_i^n = H^2 - 2K , \tag{6.5}$$

where $H = \text{tr}\{\Omega_k^i\}$ is the mean curvature and $K = \det\{\Omega_k^i\}$ is the Gaussian curvature. Our final expression for the continuum limit is

$$F_b = \tfrac{1}{2}\kappa \int dS (H^2 - 2K) . \tag{6.6}$$

This is nothing but the Helfrich energy (4.2) with bending rigidity κ and Gaussian rigidity $\kappa_G = -\kappa$. The relationship between κ and the microscopic parameter $\tilde{\kappa}$ is most easily derived by bending a triangular lattice into the shape of a cylinder. The sum in (6.1) can then be calculated by hand easily, and compared with the integral in (6.6). This procedure yields[20]

$$\kappa = \frac{\sqrt{3}}{2}\tilde{\kappa} . \tag{6.7}$$

Buckled positive and negative disclinations are depicted in Fig. 5. A check with the inextensional calculations of Sec. IV results from simulating a positive disclination with $K_0/\tilde{\kappa}$ so large that R_b is much less than a lattice spacing. Figure 6 is a semilogarithmic plot of F/κ versus R for buckled positive and negative disclinations with $K_0/\tilde{\kappa} = 2000$. The energies behave like

$$F_b = 1.159\kappa \ln\left[\frac{R}{a}\right] \tag{6.8a}$$

for positive disclinations and

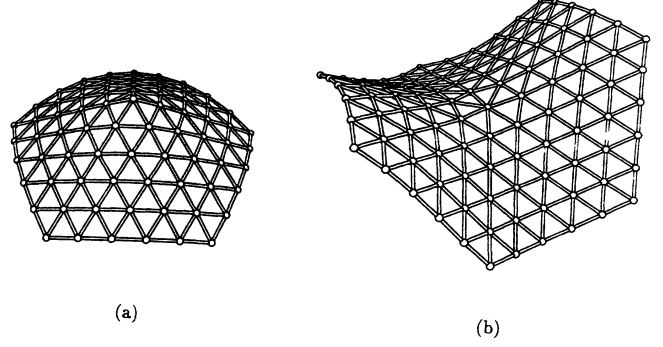$$F_b = 2.276\kappa \ln\left[\frac{R}{a}\right] \tag{6.8b}$$

(a)   (b)

FIG. 5. (a) Buckled positive disclination $(K_0/\tilde{\kappa} = 2000)$. (b) Buckled negative disclination $(K_0/\tilde{\kappa} = 2000)$.

for negative disclinations. The positive disclination result agrees with (4.24) very well, and the negative disclination result is only about 10% less than the upper bound (4.26). In Fig. 7 are graphed the energies of buckled disclinations versus R for various values of $K_0/\tilde{\kappa}$. Each curve branches off from the flat disclination curve at the critical buckling radius R_b. The smooth way these curves join onto the flat disclination curve suggests a weakly first-order or possibly continuous buckling transition. Figure 8 shows that the radii of buckling are linear in $\sqrt{\kappa/K_0}s$ [as predicted in (5.7b)], with slopes
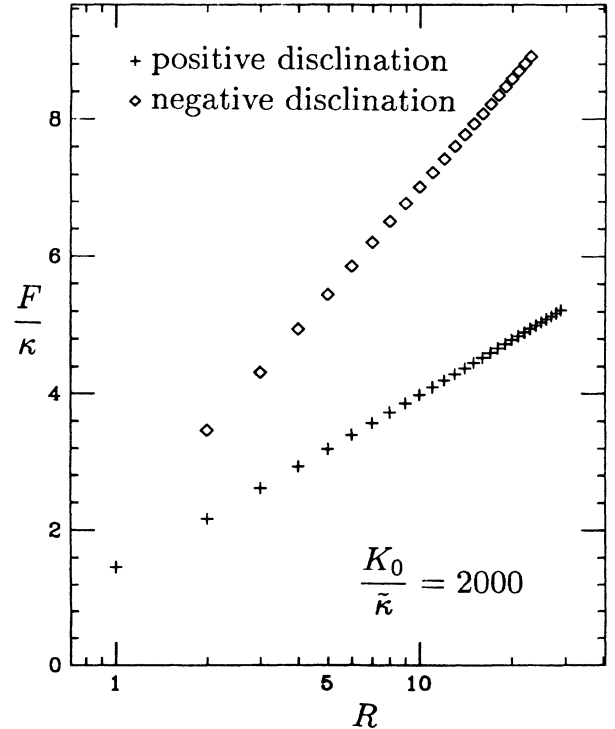

FIG. 6. Semilogarithmic plot of energy (in units of κ) vs R for buckled disclinations. Here $K_0/\tilde{\kappa} = 2000$, which places these systems in the inextensional limit.
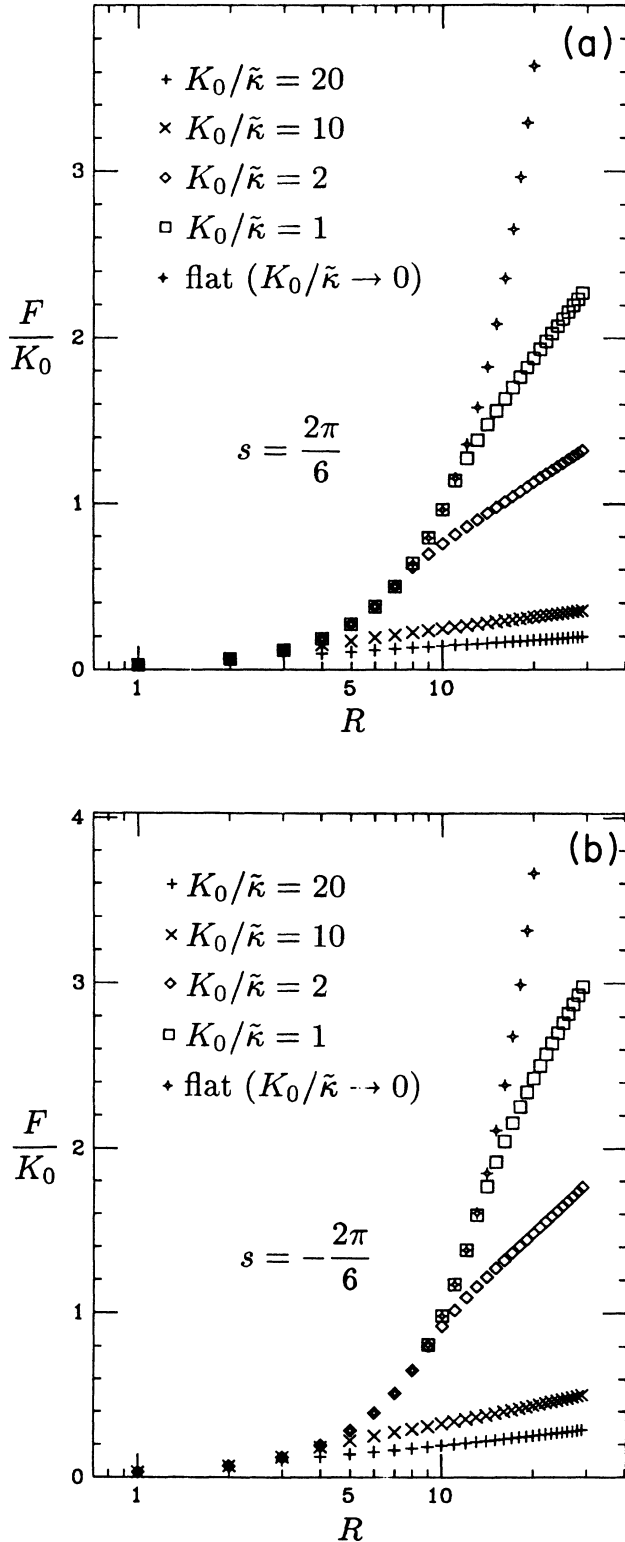
FIG. 7. Semilogarithmic plot of energy (in units of K_0) vs R for buckled positive (a) and negative (b) disclinations. The flat disclination energy is also plotted for comparison. For every value of $K_0/\tilde{\kappa}$, the graph of the buckled disclination energy separates from the flat disclination energy at some critical radius R_b.

$$R_b\left[\frac{K_0 s}{\kappa}\right]^{1/2}=13.0\pm1.0 \qquad (6.9a)$$

for positive disclinations

$$R_b\left[\frac{K_0 s}{\kappa}\right]^{1/2}=14.2\pm1.0 \qquad (6.9b)$$

for negative disclinations. These results are in rough agreement with the continuum Mitchell-Head bounds (5.10), obtained using (2.19b), which as stated before are somewhat inaccurate for disclinations.

The curves in Fig. 7 all become logarithmic beyond the buckling radius, which indicates that the inextensional limit is reached for large R. This notion can be made more precise through scaling arguments. Let us divide the membrane into the regions $0 \leq r \leq R_b$ and $R_b \leq r \leq R$, where R_b is the radius of buckling. Let $F_{in}(\kappa,K_0)$ be the energy of the inner region, and $F_{out}(R,\kappa,K_0)$ the energy of the outer region. Given some solution of the von Kármán equations for the parameters κ and K_0, rescale it via (5.3) with $\tau=\lambda^2$. Then the disclinicity s is left unchanged, and

$$F_{out}(R,\kappa,K_0)=F_{out}\left[\lambda R,\kappa,\frac{K_0}{\lambda^2}\right]. \qquad (6.10)$$

Suppose R is much greater than the critical buckling radius R_b associated with the left-hand side of (6.10). We then choose $\lambda=R_b/R \ll 1$ and see from the right-hand side that this system is equivalent to one of smaller size, but with an enormous elasticity parameter $K_0 R^2/R_b^2$. Thus membranes are effectively in the inextensional limit for large R. Assuming the inextensional limit applies for
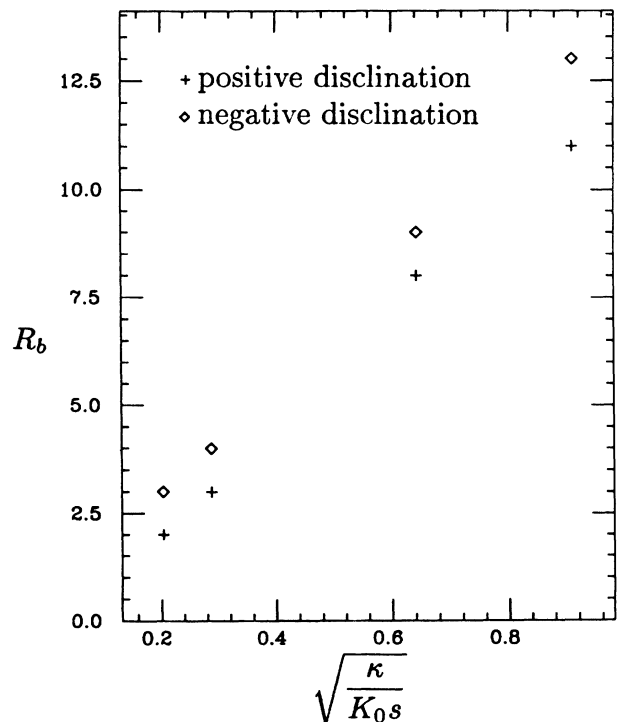

FIG. 8. Radius of buckling vs $\sqrt{\kappa/K_0 s}$ for disclinations.

all $R > R_b$, we would expect

$$F(R,\kappa,K_0) \approx \begin{vmatrix} 1.159 \\ 2.276 \end{vmatrix} \kappa \ln \left| \frac{R}{R_b} \right| + F_{in}(\kappa,K_0) , \qquad (6.11)$$

where the numerical constants for positive and negative disclinations have been taken from (6.8). A crude approximation for F_{in} can be obtained from the energy of a flat disclination of size R_b,

$$F_{in}(\kappa,K_0) \approx \frac{K_0 s^2}{32\pi} R_b^2 \approx \kappa \frac{|s| y_c^2}{32\pi} . \qquad (6.12)$$

So F_{in} is just κ times a constant of order unity. In Fig. 9 F/κ has been plotted versus the rescaled variable R/R_b for buckled positive disclinations, showing that F/κ is indeed a function only of R/R_b, as suggested by Eqs. (6.11) and (6.12).

Two views of a buckled dislocation are shown in Fig. 10. When the energies are plotted on a semilogarithmic scale as in Fig. 11(a), the slope of each curve is monotonically decreasing. This means that the energy of a buckled dislocation diverges slower than any logarithm. Because the entropy of an isolated dislocation still diverges logarithmically, this result suffices to show that dislocations will be unbound at any finite temperature. We make the stronger conjecture that the energies asymptotically approach finite constants as $R \to \infty$, which Fig. 11(b) makes plausible. The buckling radii versus κ/K_0 for a dislocation are graphed in Fig. 12. The plot is approximately
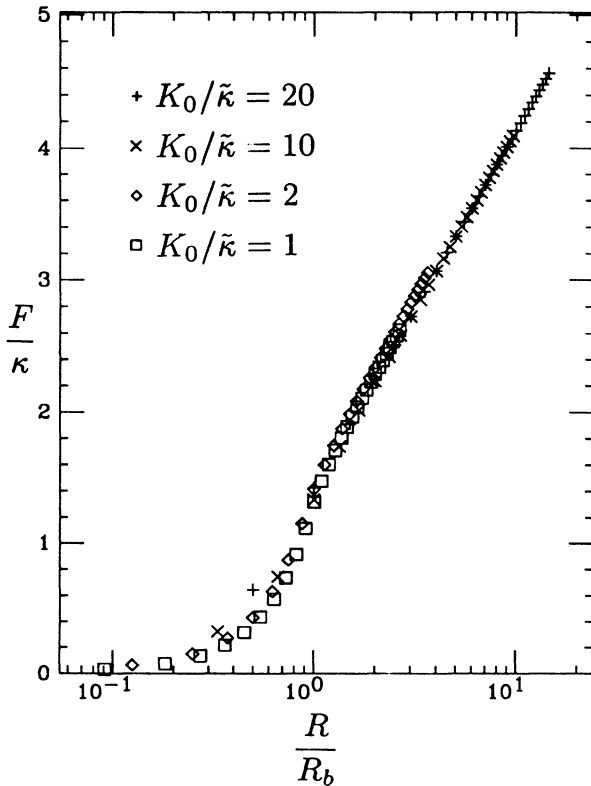
linear as expected from (5.7a). To compare with the Mitchell-Head results we extract a slope from the two points at large R, which are most likely to give a good approximation to the continuum limit,

$$R_b \frac{K_0 b}{\kappa} = 127 \pm 10 , \qquad (6.13)$$

where the error is estimated from the scatter in the remaining points. The agreement with Eq. (5.10c) is rather good.

From the assertion that the dislocation energies are finite a great deal of information can be extracted by scaling arguments. Using (5.3) with $\lambda = \tau$ leaves b invariant and transforms the energy in the region $R_1 < r < R_2$,

$$F(R_1,R_2,\kappa,K_0) = F(\lambda R_1,\lambda R_2,\lambda\kappa,K_0) . \qquad (6.14)$$

We apply this relation to inextensional dislocations of infinite size and unit Burgers vector. It follows from (4.16) that the total energy must be given by

$$F(a,\infty,\kappa,K_0) \approx \kappa \Phi_\infty , \qquad (6.15)$$

where $\Phi_\infty = \lim_{R \to \infty} \Phi(\kappa_G/\kappa,R)$ is a universal constant, independent of κ_G/κ and other elastic parameters. The function $\Phi(\kappa_G/\kappa,R)$ was defined in Eq. (4.16). The energy in the region outside some radius R can be transformed into the total energy of a dislocation with a different rigidity $\kappa' = (a/R)\kappa$ by choosing $\lambda = a/R$ in (6.14),

$$F(R,\infty,\kappa,K_0) = F(\lambda R,\infty,\lambda\kappa,K_0) = F\left[a,\infty,\frac{a}{R}\kappa,K_0\right]$$
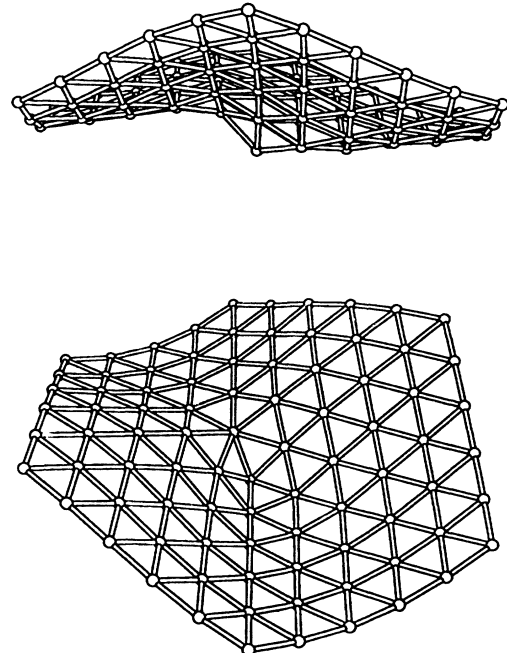
$$\approx \frac{a}{R}\kappa\Phi_\infty . \qquad (6.16)$$

FIG. 9. Positive disclination energies vs the rescaled variable R/R_b.

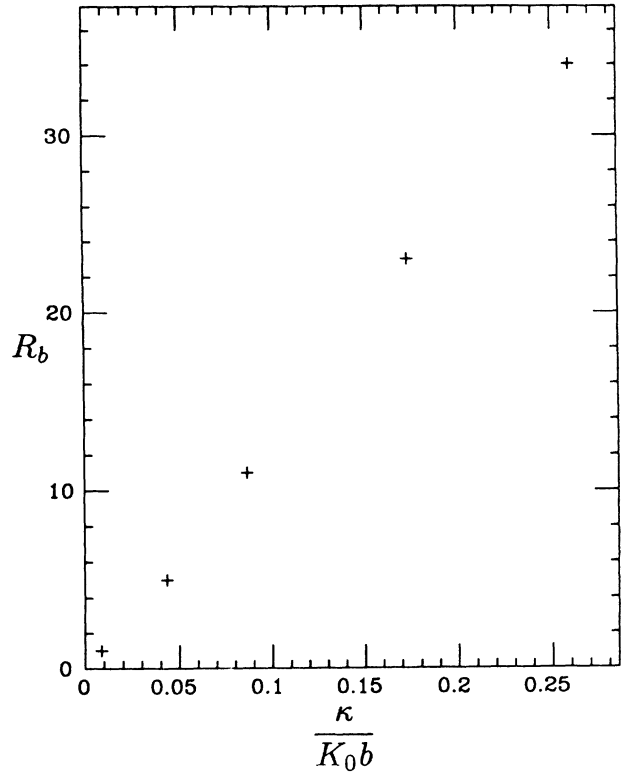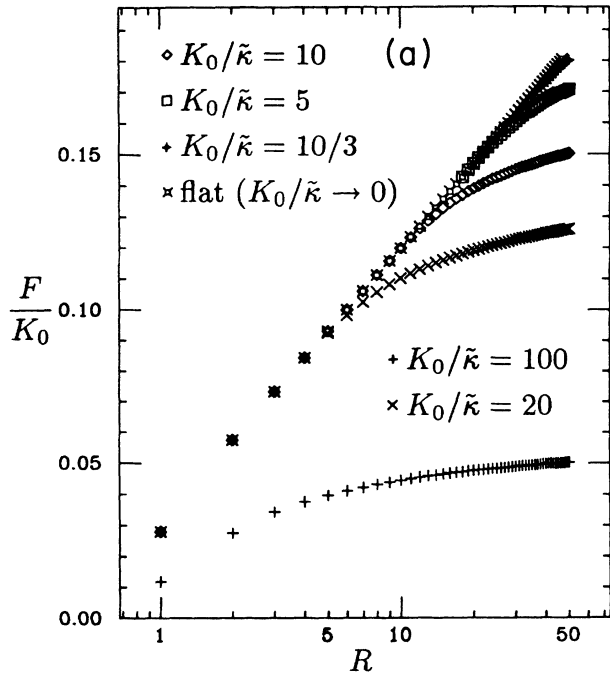FIG. 10. Two views of a buckled dislocation with $K_0/\tilde{\kappa} = 100$.

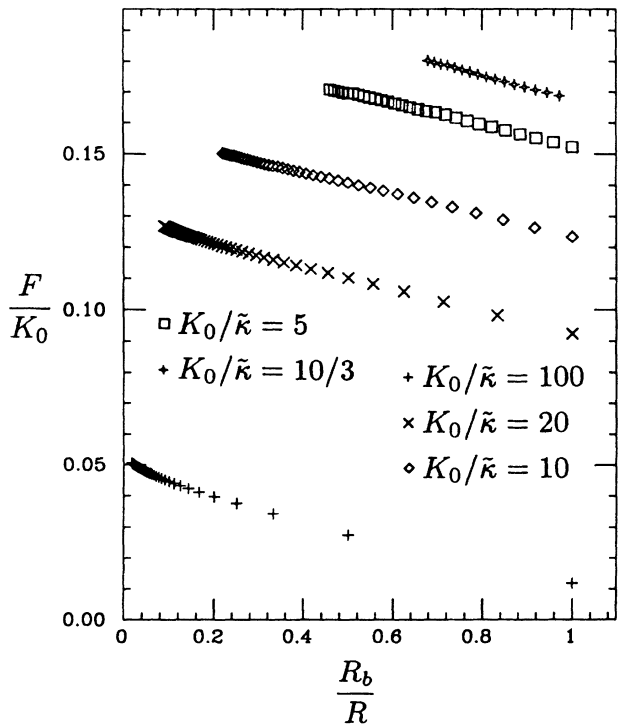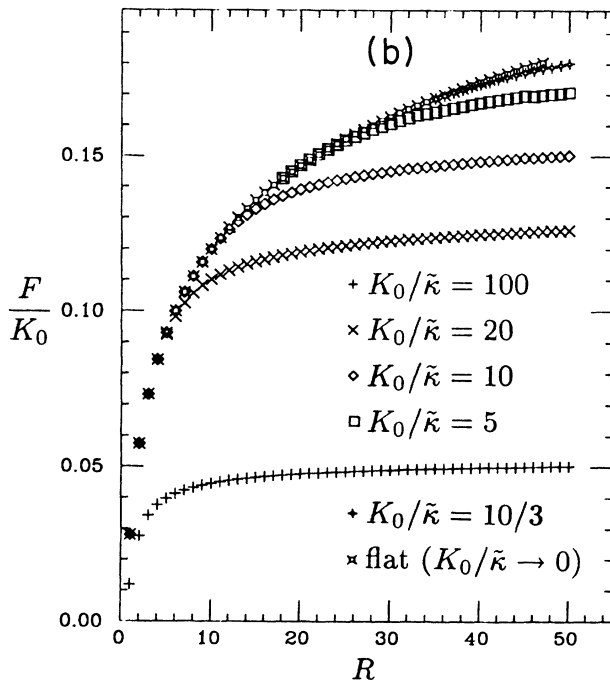FIG. 12. Radius of buckling vs $\kappa/K_0 b$ for dislocations.

FIG. 11. Semilogarithmic (a) and regular (b) plots of energy (in units of K_0) vs R for buckled dislocations with unit lattice spacing and Burgers vector. The flat dislocation energy is also plotted for comparison.

FIG. 13. Dislocation energies (in units of K_0) plotted vs R_b/R.

Since the rescaling has taken the system even further into the inextensional regime $[R_b' = (a/R)R_b]$, the last approximation is a good one. Then the energy in the region inside R is given by

$$F(a,R,\kappa,K_0) = F(a, \infty, \kappa, K_0) - F(R, \infty, \kappa, K_0)$$

$$\approx \kappa\Phi_\infty - \frac{a}{R}\kappa\Phi_\infty \ . \tag{6.17}$$

We can now argue as we did for disclinations that dislocations behave as if they were inextensional for sufficiently large R. Thus the energy of a dislocation, if bounded, should approach some finite value F_∞ with a $1/R$ dependence, as in (6.17). In the general case we expect that

$$\frac{F}{K_0 b^2} \approx \frac{F_\infty}{K_0 b^2} - \frac{\Phi_\infty}{x_c}\frac{R_b}{R} \ , \tag{6.18}$$

where x_c is the coefficient of proportionality in (5.7a). The factors in the $1/R$ correction are arranged to give agreement with the inextensional prediction (6.17). This

prediction is checked in Fig. 13, which is a graph of dislocation energies F/K_0 versus R_b/R. All curves do indeed have approximately the same slope, as predicted by Eq. (6.18). We can approximate F_∞ by the energy of a flat dislocation of radius R_b,

$$\frac{F_\infty}{K_0 b^2} \approx \frac{1}{8\pi}\ln\left[\frac{R_b}{a}\right] + c\left[\frac{\kappa_G}{\kappa}\right] \ , \tag{6.19}$$

where the dimensionless function c has been added to account for the energy F_{out} outside the radius of buckling.

ACKNOWLEDGMENTS

[1]J. M. Kosterlitz and D. J. Thouless, J. Phys. C 5, 124 (1972); 6, 1181 (1973).

[2]D. R. Nelson and B. I. Halperin, Phys. Rev. B 19, 2457 (1979).

[3]See, e.g., Physics of Amphiphilic Films, edited by D. Langevin and J. Meunier (Springer, Berlin, 1987).

[4]J. Larche, J. Appell, G. Porte, P. Bassereau, and J. Marignan, Phys. Rev. Lett. 56, 1700 (1986); C. R. Safinya, D. Roux, G. S. Smith, S. K. Sinha, P. Dimon, N. A. Clark, and A. M. Bellocq, ibid. 57, 2718 (1986).

[5]W. F. Harris, in Surface and Defect Properties of Solids, Specialist Periodical Reports (The Chemical Society, London, 1973), Vol. 3.

[6]D. R. Nelson and L. Peliti, J. Phys. (Paris) 48, 1085 (1987).

[7]L. D. Landau and E. M. Lifshitz, Theory of Elasticity (Pergamon, New York, 1970).

[8]L. H. Mitchell and A. K. Head, J. Mech. Phys. Solids 9, 131 (1961).

[9]E. G. Coker and L. N. G. Filon, A Treatise on Photo-Elasticity (Cambridge University Press, Cambridge, 1931).

[10]E. Kröner, in Physics of Defects, edited by R. Balian, M. Kléman, and J.-P. Poirier (North-Holland, Amsterdam, 1981), pp. 235–243.

[11]F. R. N. Nabarro, Theory of Crystal Dislocations (Clarendon,

Oxford, 1967), pp. 46–52.

[12]S. Sachdev and D. R. Nelson, J. Phys. C 17, 5473 (1984).

[13]This corrects the assertion in Ref. 6 that the energy of an isolated disclination increases like $R^2\ln(R/a)$.

[14]See, for example, Appendix C of D. R. Nelson, Phys. Rev. B 26, 269 (1982).

[15]We focus on the triangular lattice for simplicity, and because it obeys isotropic elasticity theory (Ref. 7).

[16]W. H. Press, B. P. Flannery, S. A. Teukolsky, and W. T. Vetterling, Numerical Recipes (Cambridge University Press, Cambridge, 1986), Chap. 10.

[17]W. Helfrich, Z. Naturforsch. 28c, 693 (1973). We adopt the convention that the mean curvature be the sum of the principal curvatures, rather than the average.

[18]B. A. Dubrovin, A. T. Fomenko, and S. P. Novikov, Modern Geometry (Springer, New York, 1984), Vol. 1.

[19]T. von Kármán, Festigkeitsprobleme im Maschinenbau, in Collected Works, (Butterworths, London, 1956), Vol. 1, p. 177; A. Föppl, Vorlesungen über technische Mechanik (B. G. Teubner, Leipzig, 1907), Vol. 5, p. 132.

[20]Y. Kantor and D. R. Nelson, Phys. Rev. Lett. 58, 2774 (1987); Phys. Rev. A 36, 4020 (1987). The coefficient relating κ and $\bar{\kappa}$ is given incorrectly in this paper.